Published in final edited form as:
J Neurosci Res. 2013 February ; 91(2): 240–248. doi:10.1002/jnr.23150.

N-Methyl-*D*-Aspartate Receptor-Mediated Axonal Injury in Adult Rat Corpus Callosum

Jingdong Zhang, **Jianuo Liu**, **Howard S. Fox**, and **Huangui Xiong**★
Department of Pharmacology and Experimental Neuroscience, University of Nebraska Medical Center, Omaha, Nebraska

Abstract

Damage to white matter such as corpus callosum (CC) is a pathological characteristic in many brain disorders. Glutamate (Glut) excitotoxicity through AMPA receptors on oligodendrocyte (OL) was previously considered as a mechanism for white matter damage. Recent studies have shown that *N*-methyl-*D*-aspartate receptors (NMDARs) are expressed on myelin sheath of neonatal rat OL processes and that activation of these receptors mediated demyelization. Whether NMDARs are expressed in the adult CC and are involved in excitotoxic axonal injury remains to be determined. In this study, we demonstrate the presence of NMDARs in the adult rat CC and their distributions in myelinated nerve fibers and OL somata by means of immunocytochemical staining and Western blot. Incubation of the CC slices with Glut or NMDA induced axonal injury as revealed by analyzing amplitude of CC fiber compound action potentials (CAPs) and input–output response. Both Glut and NMDA decreased the CAP amplitude and input–output responses, suggesting an involvement of NMDARs in Glut- and NMDA-induced axonal injury. The involvement of NMDAR in Glut-induced axonal injury was further assayed by detection of β-amyloid precursor protein (β-APP) in the CC axonal fibers. Treatment of the CC slices with Glut resulted in β-APP accumulation in the CC fibers as detected by Western blot, reflecting an impairment of axonal transport function. This injurious effect of Glut on CC axonal transport was significantly blocked by MK801. Taken together, these results show that NMDARs are expressed in the adult CC and are involved in excitotoxic activity in adult CC slices in vitro.

Keywords

NMDA receptor; excitotoxicity; myelinated fibers; oligodendrocyte; corpus callosum

It has been recognized in recent years that central white matter abnormalities play an important role in the pathogenesis of neurological disorders, such as Alzheimer's disease (AD; Frederiksen et al., 2011) and human immunodeficiency virus type-1 (HIV-1)-associated neurocognitive disorders (HAND; Navia et al., 1986; Gongvatana et al., 2009; Wohlschlaeger et al., 2009). The corpus callosum (CC), the unique white matter structure bridging bilateral hemispheres, has been well documented for its involvement in a variety of neurological disorders. For example, significant CC atrophy, which was independent of age-related white matter changes, could be detected in patients with mild AD, and the detected CC atrophy was correlated with cognitive decline in AD patients (Frederiksen et al., 2011). In AIDS patients with HAND, a striking pathological feature is subcortical white matter damage (Navia et al., 1986; Gongvatana et al., 2009; Wohlschlaeger et al., 2009), and the

★Correspondence to: Huangui Xiong, MD, PhD, Department of Pharmacology and Experimental Neuroscience, University of Nebraska Medical Center, 985215 Nebraska Medical Center, Omaha, NE 68198-5880. hxiong@unmc.edu.

CC abnormality has been demonstrated by studies of pathology (Navia et al., 1986; Bell, 1998; Masliah et al., 2000; Gongvatana et al., 2009; Wohlschlaeger et al., 2009), magnetic resonance imaging (Stout et al., 1998), and diffusion tensor imaging (Navia et al., 1986; Chen et al., 2009; Gongvatana et al., 2009; Wohlschlaeger et al., 2009). In addition, the progression of CC atrophy has also been found in multiple sclerosis (Yaldizli et al., 2011), progressive supranuclear palsy (Ito et al., 2008), Parkinson's disease (Wiltshire et al., 2005; Boelmans et al., 2010), primary lateral sclerosis (Tartaglia et al., 2009), shaken baby syndrome (Bonnier et al., 2002, 2004), and Williams's syndrome (Tomaiuolo et al., 2002).

Although the CC abnormalities have been observed in many neurological disorders, the mechanisms underlying the CC white matter damage remain elusive. It is well known that damage of the myelin sheath formed by oligodendrocytes (OL) is a characteristic of many CNS disorders. Thus, dysfunction or injury of OLs may contribute to the CC white matter damage. Early studies have revealed that OLs were vulnerable to glutamate (Glut)-mediated toxicity (Oka et al., 1993; Matute et al., 1997), and this Glut-associated excitotoxicity in OLs was believed to be mediated only by AMPA and kainate receptors (Patneau et al., 1994; Garcia-Barcina and Matute, 1998; Matute et al., 2001; Tekkok and Goldberg, 2001; Dewar et al., 2003; Stys, 2004). However, recent studies have shown that *N*-methyl-*D*-aspartate receptors (NMDARs) are expressed on the myelin sheath of OL processes, and activation of these receptors during ischemia resulted in myelin damage in neonatal CC and optical nerve (Karadottir et al., 2005; Salter and Fern, 2005; Micu et al., 2006). As NMDAR expression is subject to developmental change (Monyer et al., 1994; Cull-Candy et al., 2001), whether the mature OLs with their processes of myelin sheath continue to express NMDAR in adult rat CC and whether these NMDARs in the adult CC mediate axonal injuries are still unknown. In the present work, we studied expression and distribution of NMDAR subunit 1 (NMDAR1) in the CC of adult rats, because functional NMDARs are multimeric assemblies composed of at least one obligatory NMDAR1 (Seeburg, 1993; Ozawa et al., 1998; Dingledine et al., 1999). We also determined whether the NMDARs expressed in the CC are functional by examination of Glut or NMDA alteration of the CC fiber compound action potentials (CAPs; Crawford et al., 2009) and input–output responses and by evaluation of MK801 blockade of Glut excitotoxicity, which was determined by accumulation of β-amyloid precursor protein (β-APP) in the CC fibers (Medana and Esiri, 2003). These results demonstrated that functional NMDARs are expressed in the CC of adult rats and are involved in Glut excitotoxicity.

MATERIALS AND METHODS

Chemicals and Reagents

NMDA, (+)-MK-801 hydrogen maleate (MK801), L-glutamic acid monosodium salt hydrate (Glut), and chemicals used for making artificial cerebrospinal fluid (ACSF) were purchased from Sigma-Aldrich (St. Louis, MO). Stock solutions of NMDA (100 mM), glutamate (100 mM), and MK801 (10 mM) were made individually using double-distilled H_2O, and aliquots were stored in a −20°C freezer (NMDA and MK801) or a regular (4°C) refridgerator (glutamate). They were diluted to desired concentrations in ACSF on the experimental day and applied to the CC slices for pre-treatment before electrophysiological recording. The sources for specific antibodies and other reagents used in the experiments are indicated in the text.

Animals

In total 34 healthy Sprague-Dawley rats of either sex (25–40 days old; Charles River Laboratories, Wilmington, MA) were used in this study. Western blotting was performed in 30–35-day-old rats of either sex of two groups: 1) eight rats for detecting NMDAR1

expression in CC and 2) seven male rats for examine β-APP accumulation after Glut treatment. Twelve rats (30–40 days old) of either sex were used for immunocytochemical staining. Electrophysiological experiments were carried out with seven male rats (25–35 days old). All experimental protocols and animal care were carried out in accordance with the National Institutes of Health *Guide for the care of laboratory animals in research* and approved by the Institutional Animal Care and Use Committee of the University of Nebraska Medical Center (IACUC 00-062-07-EP). All efforts were made to minimize animal suffering and the number of animals used in the study.

Preparation and Incubation of Brain Slices

Animals were anesthetized with isoflurane and decapitated. Brains were quickly removed from the cranial cavity and placed into an ice-cold (4°C), oxygenated ACSF contained (in mM): NaCl 124.0, KCl 3.0, $CaCl_2$ 2.0, $MgCl_2$ 2.0, NaH_2PO_4 1.25, $NaHCO_3$ 26.0, and glucose 10.0. The ACSF was equilibrated with 95% O_2 and 5% CO_2 and had a pH of 7.4–7.5. Coronal brain slices containing the CC (500 μm in thickness) were cut using an NVSLM1 Vibroslicer (WPI, Sarasota, FL). The slices were divided into either control (Ctrl) vs. Glut- or Ctrl vs. NMDA-treated groups in each rat in electrophysiological experiments (for further details see below under Electrophysiology). For immunofluorescent staining, slices were transferred into 4% paraformaldehyde in 0.1 M phosphate buffer (PB; pH 7.4) immediate after cutting and fixed overnight at 4°C. The slices were then immersed in 10%, 20%, and 30% sucrose in PB and finally in OCT, and then 10-μm-thick frozen sections were cut with a cryostat. Sections were mounted on slides and kept in a −20°C freezer until immunofluorescent staining was performed. The slices for Western blotting were divided into four groups: 1) detection of NMDAR1, the tissues from basal ganglion (BG), CC, cortex (Ctx), and hippocampus (Hip) were dissected out and moved to extracting solution immediately; 2) control (Ctrl), incubation in ACSF at room temperature (RT) and continuously oxygenated with 95% O_2 and 5% CO_2 for 13 hr (the same for groups 3 and 4); 3) Glut-treated, incubation in ACSF with 50 μM Glut; and 4) Glut + MK801, incubation in ACSF with 50 μM Glut and 20 μM MK801.

Immunofluorescent Staining

The slides mounted with 10-μm sections were immunoblocked with 10% normal goat serum in 0.01 M phosphate-buffered saline (PBS; pH 7.2–7.4) containing 0.5% Triton X-100 at RT for 1 hr. Then, mouse anti-NMDAR1 (1:100; Invitrogen, Camarillo, CA) was used for incubation of sections at RT overnight. Rabbit antimicrotubule-associated protein 2 (MAP2; 1:500; Chemicon, Temecula, CA), antiglial fibrillary acidic protein (GFAP; 1:200; Golden Bridge Inc., Mukilteo, WA), antioligodendrocyte specific protein (OSP; 1:100; Abcam, Cambridge, MA), antineuronal nuclei (NeuN; 1:200; Millipore, Temecula, CA), and rat antimyelin basic protein (MBP; 1:200; Millipore) were used for double labeling after NMDAR1 immunostaining. The sections were incubated with primary antibodies for about 3 hr, and then Alexa Fluor 488- or 594-conjugated anti-mouse, -rabbit, or -rat (Molecular Probes, Eugene, OR) antibodies were used for immunofluorescent staining. Control slides for NMDAR1 were stained with anti-mouse without primary antibodies. All slides were finally sealed by Vectashield with DAPI (Vector, Burlingame, CA) and examined with Nikon-800 and Zeiss confocal microscopes (Zeiss LSM 510).

Electrophysiology

Experiments were carried out on the CC-containing slices prepared from male rats (25–35 day) as described above. In one group of rats (n = 4), slices were divided into Ctrl and Glut (100 μM)-treated rats; in the other group of animals (n = 3), slices were divided into Ctrl and NMDA (100 μM)-treated rats. The slices were incubated in ACSF containing Glut or NMDA for about 4 or 5 hr, respectively, before recording. For each experiment of field

potential recording, the CC-containing slice was transferred to a recording chamber and superfused with ACSF at a constant flow rate of 1.5–2.0 ml/min. The temperature of the ACSF was maintained at 30°C ± 1°C with an automatic controller (Warner Instrument, Hamden, CT). The CC fiber CAPs were evoked by constant-current stimulation (0.1–0.5 mA, 40-μsec duration, 0.2 Hz) via a bipolar Tungsten stimulating electrode. The recording electrodes, made from borosilicate glass capillaries (1.5/0.84 OD/ID; WPI) and filled with 2 M NaCl (impedance 1–4 MΩ), were placed 1–1.5 mm away from the stimulating site. Signals were amplified through an Axopatch 1D amplifier (Axon Instruments, Union City, CA) and a Dagan EX4-400 amplifier (Dagan, Minneapolis, MN), filtered at 1 kHz, digitized at 5 kHz with a Digidata 1440A interface (Axon Instruments), and recorded on a Dell computer with pCLAMP 10.1 software (Axon Instruments).

Western Blotting

The selected slices were incubated in ACSF oxygenated 95% O_2 and 5% CO_2 at room temperature until the tissues of BG, CC, Ctx, and Hip were dissected out for NMDAR1 blotting under an anatomical microscope. For β-APP blotting, only the CC tissue was dissected. Approximately 0.1 g tissue from each part of the brain was transferred in 1 ml Tissue Extraction Reagent 1 (FNN0071; Invitrogen) with 1:1,000 protease inhibitor (P-2714; Sigma-Aldrich) and homogenized. Protein concentrations were determined by using the BCA method with bovine serum albumin as a standard. The homogenate was subjected to 10% sodium dodecyl sulfate-polyamide gel electrophoresis and then transferred to a polyvinylidene difluoride (PVDF) membrane. The membranes were then blocked with 5% nonfat milk in Tris-buffered saline-Tween 20 (TBST) and incubated with either monoclonal mouse anti-NMDAR1 (1:200; Invitrogen) or rabbit polyclonal anti-NMDAR1 (1:250–500; Abcam, Cambridge, MA) in group 1 and with polyclonal rabbit anti-β-APP antibody (1:800; Millipore) in groups 2–4, followed by horseradish peroxidase (HRP)-conjugated secondary antibody (1:5,000; Jackson Immunoresearch, West Grove, PA). For gel loading control, mouse anti-β-actin (1:5,000; Sigma-Aldrich) was used to incubate PVDF membrane, followed by HRP-conjugated anti-mouse (1:5,000–10,000; Jackson Immunoresearch). Immunoreactive bands were detected using enhanced chemiluminescence and developed with autoradiograph film.

Statistical Analysis

Protein density ratio of β-APP/β-actin in each running sample was measured in Image J (NIH, Bethesda, MD) and collected for statistical analyses. One-way ANOVA multiple comparisons were assumed to process data from Ctrl, Glut, and Glut + MK801 groups. Electrophysiological data were processed in Origin 8 (OriginLab, Northampton, MA) and expressed as mean ± SEM. Student's *t*-tests were used to determine significance between experimental groups. $P \leq 0.05$ was considered significant.

RESULTS

Expression of NMDAR1 in the CC of Adult Rats

Immunoreactivity for NMDAR1 was observed in the frontal (between cortex and basal ganglion) and parietal (between cortex and hippocampus) CC (Fig. 1A–C). As a positive control, anti-NMDAR1-labeled hippocampal neurons were seen explicitly in the CA1 region (Fig. 1A, arrow), a labeling model for NMDAR immunocytochemistry (Ozawa et al., 1998). In the CC, NMDAR1-like immunoreactivities were either located in soma-like structures (Fig. 1B; arrowheads) or scattered as fiber-like structures, especially in connecting areas between CC and corona radiata (Figs. 1C, 2). In parallel, NMDAR1 proteins in the CC were also identified by Western blotting (Fig. 1D), and the band was slightly under the 100-kDa marker line, which is in the same position as the sample band given in the product data sheet

from the vendor (Abcam; ab52177). NMDAR1 proteins from BG, Ctx, and Hip were also blotted and normalized with β-actin (data not shown). The results showed that NMDAR1 density in the CC was relatively lower than the densities in the Ctx and Hip (data not shown), which is in consistent with results reported previously (Ozawa et al., 1998).

Distribution of NMDAR1 in the CC

Colocalization of NMDAR1 with MBP in the CC—NMDAR1-positive fiber-like structures and double labeling of anti-NMDAR1 and anti-MBP were observed predominantly in connection areas between the CC and the horizontal corona radiata (Fig. 2) under both confocal (Fig. 2A–O) and conventional (Fig. 2P–X) microscopes. Most of the NMDAR1-positive fiber-like structures appeared to be from dorsal or ventral borders of the horizontal corona radiata adjacent to the CC (Fig. 2A–F, S–X). In the front part of the CC, most NMDAR1-positive fiber-like labeling was from brain regions close to the cingulum (Figs. 1C, 2A–F), whereas, in the parietal part of the CC, a great deal of NMDAR1-labeled fibers appeared from the brain region around the alveus of the Hip (Fig. 2S–X). The NMDAR1-positive and NMDAR1-MBP double-labeled fiber-like structures were distributed mainly in the conjunction region between the CC and the horizontal corona radiata; these fiber-like structures tend to occur in a cluster rather than being evenly distributed (Fig. 2). There were few NMDAR1-positive fiber-like and double-labeled fiber-like structures in the central part of the CC in the coronal planes.

Colocalization of NMDAR1 and OL in the CC—To examine whether NMDAR1 was present on OL, the NMDAR1 distribution was determined as described above, and OL were labeled with anti-OSP. The double-labeled somata, though not abundant, were found in the CC. In total 54 anti-OSP-labeled somata were observed among 12 sections from six slices, including four frontal CC and two parietal CC, and six of 54 cells were double immunostained by both anti-NMDAR1 and anti-OSP under conventional microscopy and were observed in four sections of the six slices. Figure 3 is representative of colocalization of NMDAR1 and OL, which displays the somata double labeled with anti-NMDAR1 (Fig. 3A, D, arrows) and anti-OSP (Fig. 3B, E, arrowheads) under confocal microscopy. These results showed that about 11% of anti-OSP-labeled OL in the CC express NMDAR1 and are scattered in both frontal and parietal parts of the CC.

Lack of colocalization of NMDAR1 with neuronal and astrocyte somata in the CC—NeuN-or MAP2-labeled neuronal somata were distributed in the frontal and parietal parts of the CC (Fig. 4A–C) but seldom in the genu of the CC. In total 37 NeuN-positive somata (Fig. 4A, B) were observed in 12 sections from six slices (four frontal CC and two parietal CC) by counting the total number of labeled cells in the CC. With the same method of counting, we also observed a total of 23 anti-MAP2-labeled somata (Fig. 4C) in another set of 12 adjacent sections. Anti-NMDAR1 in these two sets of sections (those immunostained with either NeuN or MAP2, 24 sections in total) revealed a total of 68 anti-NMDAR1-labeled somata (Fig. 4D). However, neither NeuN nor MAP2 labeling was colocalized with NMDAR1-positive somata when examined under both conventional and confocal microscopes. Interestingly, though not labeled by neuronal markers, some anti-NMDAR1-labeled somata exhibited fairly extensive processes (Fig. 4D, arrowheads). Although numerous astrocytes were labeled by anti-GFAP in the CC (data not shown), definite GFAP and NMDAR1 double-labeled soma was not observed.

Decrease of CC Fiber CAP Amplitude With Glut or NMDA Treatment

The CC fiber CAPs were evoked by constant-current stimulation of contralateral CC (Fig. 5A, C), and input–output response curves were generated by stimuli from 0.10 to 0.45 or 0.50 mA, with an increment of 0.05 mA (Fig. 5A–D). The amplitude of CAPs was measured

according to an earlier report (Crawford et al., 2009), and data were statistically processed and plotted in Origin 8 software (Fig. 5B, D). As shown in Figure 5, the amplitudes of evoked CAPs were significantly decreased in the CC slices pretreated with Glut or NMDA.

Blockade of Glut-Induced CC Axonal Injury by MK801

Accumulation of β-APP is a sensitive indicator for functional impairment of the axons, because functional impairment decreases axoplasmic movement, resulting in β-APP accumulation in axoplasma during its fast transport from soma to terminal (Buxbaum et al., 1998; Kaether et al., 2000). To determine whether the NMDAR1 expressed in the CC is involved in Glut-induced axonal injury, we examined the protective effects of MK801 on Glut-induced axonal injury in the CC. After incubation of the CC slices with ACSF alone (Ctrl), Glut (50 μM), or Glut (50 μM) + MK801 (20 μM), a higher density of β-APP in Glut-treated CC slices was detected by Western blotting (Fig. 6). The bands (Fig. 6A) were in conformity with the molecular weight of ~ 90 kDa given in the product data sheet from the vendor. One-way ANOVA revealed significant differences between Ctrl and Glut groups ($n = 6$, $P < 0.05$) and between Glut and Glut + MK801 groups ($n = 6$, $P < 0.05$) but not between Ctrl and Glut + MK801 groups (Fig. 6B). These results indicate involvement of NMDARs in Glut-mediated axonal impairment in the CC.

DISCUSSION

The expression of NMDAR subunits exhibited distinct patterns at different developmental stages (Xia et al., 1995; Molnar et al., 2002; Tang and Carr, 2007). It has been reported that functional NMDARs are expressed on OLs in the CC of neonatal rats (Karadottir et al., 2005). Whether the NMDARs are expressed in the adult CC tissue is important for studying white matter-associated neuropathogenesis in adulthood, insofar as white matter damage is a characteristic of many CNS diseases (Navia et al., 1986; Wiltshire et al., 2005; Gongvatana et al., 2009; Kale et al., 2009; Wohlschlaeger et al., 2009; Di Paola et al., 2010; Frederiksen et al., 2011). The present work has demonstrated that NMDARs are expressed in the adult CC, and these receptors are functional in Glut- or NMDA-induced axonal injury. As NMDAR1 is believed to be a subunit obligatory for forming native heterometric NMDARs (Monyer et al., 1992; Seeburg, 1993; Ozawa et al., 1998; Dingledine et al., 1999), the detection of NMDAR1 subunit in the CC of adult rats indicates expression of NMDARs in the adult CC. Therefore, we examined only the NMDAR1 subunit in this study.

After demonstration of NMDAR expression in the adult CC, we tried to examine the distribution of NMDAR1 in the CC of adult rats by double immunocytochemical staining. Previous studies showed that NMDARs were located predominantly in the myelin sheath and processes of the OL progenitor cells and OLs in neonatal rats (Karadottir et al., 2005; Salter and Fern, 2005). In agreement with these studies, we observed the colocalization of anti-NMDAR1 with anti-MBP and anti-OSP. The exact relationship between NMDAR1 and MBP and the ultrastructural localization of NMDAR1 might be clarified through electron microscopy. The distribution pattern of the NMDAR1-positive fibers in adult CC is interesting. These fibers were located predominantly in conjunctional areas between the CC and the horizontal corona radiata. Most of these fiber-like structures appeared to extend either from the regions close to the cingulum in front parts of the CC or from the areas around alveus of the Hip in parietal parts of the CC. This pattern stimulates us to imagine a group of fibers with dense NMDARs on their myelin sheath growing into the CC from every border and losing NMDARs as they travel more deeply into the CC. Whether there are more OL precursors around borders of the CC in adulthood requires further investigation.

The observation of NMDAR1-positive somata in the CC raises the question of what type(s) of cells they are. Because majority of neurons express NMDARs (Ozawa et al., 1998), we

attempted to determine whether neurons within the adult CC express NMDAR1. With anti-NeuN (Wolf et al., 1996) and anti-MAP2 (Riederer et al., 2004), we tried to identify neurons in the CC using each of the well-established neuronal markers together with anti-NMDAR1 to perform double immunostaining. However, no double-labeled neuronal soma was observed, implying that NMDARs might not be expressed on neuronal cells in the adult CC. In contrast, anti-OSP, an established OL marker (Jagessar et al., 2008), and anti-NMDAR1 double-labeled somata were observed under both conventional and confocal microscopy. These results suggest the existence of NMDARs in the adult OLs, although the number of double-labeled soma was relatively low, about 10% upon total OSP-positive somata counted via conventional microscopy. Interestingly, some NMDAR1-positive somata were found to have a very long process, but they were neither neurons nor OLs. The CC harbors a large amount of cycling cells (Hommes and Leblond, 1967; Dalton et al., 1968), and some of them have been demonstrated to be OL progenitor cells (Gensert and Goldman, 1997). In a recent study, Fung et al. (2011) reported that neurons in white matter migrated with some features similar to those of cycling cells described in the early literature (Hommes and Leblond, 1967; Dalton et al., 1968). Because some of the NMDAR1-positive cells observed in this study possess a similar morphology to the reported cycling cells with long process and few ramifications (Hommes and Leblond, 1967; Dalton et al., 1968), these NeuN- and MAP2-negative, NMDAR1-positive cells are presumably OL progenitor cells and/or migrating neurons; these were referred to as *white matter cycling cells* in the older literature. Nonetheless, what physiological role they could play through NMDARs in the CC and why migrating neurons but not mature neurons here expressing NMDARs are completely unknown.

To examine whether the NMDARs expressed in adult CC are functional, we tested whether incubation of the CC slices with Glut or NMDA can elicit CC white matter damage. The axon injury was determined by physiological studies showing that incubation of CC slices with either Glut or NMDA significantly reduced the input–output responses and the amplitude of the CC fiber CAPs. The axonal injury was also detected by examination of axonal transport of β-APP, a sensitive indicator for detection of axonal injury, which has been widely used in studying axonal injuries in head and spinal trauma, multiple sclerosis, ischemia, infectious disease, and HIV-1-associated white matter damage at autopsy (Medana and Esiri, 2003). This is sensitive because any functional change such as downregulation of microtubule ATPase (Brady, 1985) or calcium ion imbalance (Rivera et al., 1995) that will slacken axoplasmic movement can engender accumulation of β-APP in axoplasma during its fast transport from soma to terminal (Buxbaum et al., 1998; Kaether et al., 2000). We found that incubation of the CC slices with Glut increased the β-APP density in the CC tissue, as revealed by Western blotting. The Glut-induced increase of β-APP density was blocked by MK801, an NMDAR open channel blocker, indicating the involvement of NMDARs in Glut-induced axonal injury in the adult rat CC. However, the contribution of AMPA receptor in Glut-induced axonal injury in the adult rat CC, if any, cannot be excluded based on results of this study (Matute et al., 1997, 2001; Tekkok and Goldberg, 2001).

In summary, NMDARs are expressed in the CC of adult rats. They are distributed along myelinated nerve fibers growing into the CC and on OL somata. Activation of these receptors resulted in CC axonal damage as revealed by decreased amplitude of the CC fiber CAPs and input–output responses in addition to an impaired axonal transport of β-APP. Although the physiological role of the NMDARs in the adult CC remains to be determined, activation of these receptors under pathological conditions may play an important role in the pathogenesis of CNS disorders. In addition, our work reveals that ex vivo treatment of the CC slices with pathogenic substances (or pathogens in the future studies) and detection of the CC injury by analyzing CC fiber CAPs and axonal transport of β-APP could be an

applicable laboratory model for studying the mechanisms underlying white matter damage in many CNS disorders.

Acknowledgments

Contract grant sponsor: NIH; Contract grant number: R01 NS063878 (to H.X.); Contract grant number: P30 MH062261 (to H.S.F., H.X.).

We thank Dr. Daniel T. Monaghan for his very helpful discussion and comments on the results of Western blot detection of NMDAR NR1 subunit expression in the CC. The authors also thank Ms. Jane Kruchowsky for reading the manuscript and two anonymous reviewers for their constructive criticisms and comments.

References

Bell JE. The neuropathology of adult HIV infection. Rev Neurol (Paris). 1998; 154:816–829. [PubMed: 9932303]

Boelmans K, Bodammer NC, Suchorska B, Kaufmann J, Ebersbach G, Heinze HJ, Niehaus L. Diffusion tensor imaging of the corpus callosum differentiates corticobasal syndrome from Parkinson's disease. Parkinsonism Rel Disord. 2010; 16:498–502.

Bonnier C, Mesples B, Carpentier S, Henin D, Gressens P. Delayed white matter injury in a murine model of shaken baby syndrome. Brain Pathol. 2002; 12:320–328. [PubMed: 12146800]

Bonnier C, Mesples B, Gressens P. Animal models of shaken baby syndrome: revisiting the pathophysiology of this devastating injury. Pediatr Rehabil. 2004; 7:165–171. [PubMed: 15204568]

Brady ST. A novel brain ATPase with properties expected for the fast axonal transport motor. Nature. 1985; 317:73–75. [PubMed: 2412134]

Buxbaum JD, Thinakaran G, Koliatsos V, O'Callahan J, Slunt HH, Price DL, Sisodia SS. Alzheimer amyloid protein precursor in the rat hippocampus: transport and processing through the perforant path. J Neurosci. 1998; 18:9629–9637. [PubMed: 9822724]

Chen Y, An H, Zhu H, Stone T, Smith JK, Hall C, Bullitt E, Shen D, Lin W. White matter abnormalities revealed by diffusion tensor imaging in non-demented and demented HIV^+ patients. Neuroimage. 2009; 47:1154–1162. [PubMed: 19376246]

Crawford DK, Mangiardi M, Tiwari-Woodruff SK. Assaying the functional effects of demyelination and remyelination: revisiting field potential recordings. J Neurosci Methods. 2009; 182:25–33. [PubMed: 19481113]

Cull-Candy S, Brickley S, Farrant M. NMDA receptor subunits: diversity, development and disease. Curr Opin Neurobiol. 2001; 11:327–335. [PubMed: 11399431]

Dalton MM, Hommes OR, Leblond CP. Correlation of glial proliferation with age in the mouse brain. J Comp Neurol. 1968; 134:397–400. [PubMed: 5721158]

Dewar D, Underhill SM, Goldberg MP. Oligodendrocytes and ischemic brain injury. J Cereb Blood Flow Metab. 2003; 23:263–274. [PubMed: 12621301]

Di Paola M, Spalletta G, Caltagirone C. In vivo structural neuroanatomy of corpus callosum in Alzheimer's disease and mild cognitive impairment using different MRI techniques: a review. J Alzheimers Dis. 2010; 20:67–95. [PubMed: 20164572]

Dingledine R, Borges K, Bowie D, Traynelis SF. The glutamate receptor ion channels. Pharmacol Rev. 1999; 51:7–61. [PubMed: 10049997]

Frederiksen KS, Garde E, Skimminge A, Ryberg C, Rostrup E, Baare WF, Siebner HR, Hejl AM, Leffers AM, Waldemar G. Corpus callosum atrophy in patients with mild Alzheimer's disease. Neurodegener Dis. 2011; 8:476–482. [PubMed: 21659724]

Fung SJ, Joshi D, Allen KM, Sivagnanasundaram S, Rothmond DA, Saunders R, Noble PL, Webster MJ, Weickert CS. Developmental patterns of doublecortin expression and white matter neuron density in the postnatal primate prefrontal cortex and schizophrenia. PLoS One. 2011; 6:e25194. [PubMed: 21966452]

Garcia-Barcina JM, Matute C. AMPA-selective glutamate receptor subunits in glial cells of the adult bovine white matter. Brain Res Mol Brain Res. 1998; 53:270–276. [PubMed: 9473692]

Gensert JM, Goldman JE. Endogenous progenitors remyelinate demyelinated axons in the adult CNS. Neuron. 1997; 19:197–203. [PubMed: 9247275]

Gongvatana A, Schweinsburg BC, Taylor MJ, Theilmann RJ, Letendre SL, Alhassoon OM, Jacobus J, Woods SP, Jernigan TL, Ellis RJ, Frank LR, Grant I. White matter tract injury and cognitive impairment in human immunodeficiency virus-infected individuals. J Neurovirol. 2009; 15:187–195. [PubMed: 19306228]

Hommes OR, Leblond CP. Mitotic division of neuroglia in the normal adult rat. J Comp Neurol. 1967; 129:269–278. [PubMed: 4166505]

Ito S, Makino T, Shirai W, Hattori T. Diffusion tensor analysis of corpus callosum in progressive supranuclear palsy. Neuroradiology. 2008; 50:981–985. [PubMed: 18779957]

Jagessar SA, Smith PA, Blezer E, Delarasse C, Pham-Dinh D, Laman JD, Bauer J, Amor S, t'Hart B. Autoimmunity against myelin oligodendrocyte glycoprotein is dispensable for the initiation although essential for the progression of chronic encephalomyelitis in common marmosets. J Neuropathol Exp Neurol. 2008; 67:326–340. [PubMed: 18379435]

Kaether C, Skehel P, Dotti CG. Axonal membrane proteins are transported in distinct carriers: a two-color video microscopy study in cultured hippocampal neurons. Mol Biol Cell. 2000; 11:1213–1224. [PubMed: 10749925]

Kale N, Agaoglu J, Tanik O. Electrophysiological and clinical correlates of corpus callosum atrophy in patients with multiple sclerosis. Neurol Res. 2009; 32:886–890. [PubMed: 19825276]

Karadottir R, Cavelier P, Bergersen LH, Attwell D. NMDA receptors are expressed in oligodendrocytes and activated in ischaemia. Nature. 2005; 438:1162–1166. [PubMed: 16372011]

Masliah E, DeTeresa RM, Mallory ME, Hansen LA. Changes in pathological findings at autopsy in AIDS cases for the last 15 years. AIDS. 2000; 14:69–74. [PubMed: 10714569]

Matute C, Sanchez-Gomez MV, Martinez-Millan L, Miledi R. Glutamate receptor-mediated toxicity in optic nerve oligodendrocytes. Proc Natl Acad Sci U S A. 1997; 94:8830–8835. [PubMed: 9238063]

Matute C, Alberdi E, Domercq M, Perez-Cerda F, Perez-Samartin A, Sanchez-Gomez MV. The link between excitotoxic oligodendroglial death and demyelinating diseases. Trends Neurosci. 2001; 24:224–230. [PubMed: 11250007]

Medana IM, Esiri MM. Axonal damage: a key predictor of outcome in human CNS diseases. Brain. 2003; 126:515–530. [PubMed: 12566274]

Micu I, Jiang Q, Coderre E, Ridsdale A, Zhang L, Woulfe J, Yin X, Trapp BD, McRory JE, Rehak R, Zamponi GW, Wang W, Stys PK. NMDA receptors mediate calcium accumulation in myelin during chemical ischaemia. Nature. 2006; 439:988–992. [PubMed: 16372019]

Molnar E, Pickard L, Duckworth JK. Developmental changes in ionotropic glutamate receptors: lessons from hippocampal synapses. Neuroscientist. 2002; 8:143–153. [PubMed: 11954559]

Monyer H, Sprengel R, Schoepfer R, Herb A, Higuchi M, Lomeli H, Burnashev N, Sakmann B, Seeburg PH. Heteromeric NMDA receptors: molecular and functional distinction of subtypes. Science. 1992; 256:1217–1221. [PubMed: 1350383]

Monyer H, Burnashev N, Laurie DJ, Sakmann B, Seeburg PH. Developmental and regional expression in the rat brain and functional properties of four NMDA receptors. Neuron. 1994; 12:529–540. [PubMed: 7512349]

Navia BA, Cho ES, Petito CK, Price RW. The AIDS dementia complex: II. Neuropathology Ann Neurol. 1986; 19:525–535.

Oka A, Belliveau MJ, Rosenberg PA, Volpe JJ. Vulnerability of oligodendroglia to glutamate: pharmacology, mechanisms, and prevention. J Neurosci. 1993; 13:1441–1453. [PubMed: 8096541]

Ozawa S, Kamiya H, Tsuzuki K. Glutamate receptors in the mammalian central nervous system. Prog Neurobiol. 1998; 54:581–618. [PubMed: 9550192]

Patneau DK, Wright PW, Winters C, Mayer ML, Gallo V. Glial cells of the oligodendrocyte lineage express both kainate- and AMPA-preferring subtypes of glutamate receptor. Neuron. 1994; 12:357–371. [PubMed: 7509160]

Riederer BM, Berbel P, Innocenti GM. Neurons in the corpus callosum of the cat during postnatal development. Eur J Neurosci. 2004; 19:2039–2046. [PubMed: 15090031]

Rivera DT, Langford GM, Weiss DG, Nelson DJ. Calmodulin regulates fast axonal transport of squid axoplasm organelles. Brain Res Bull. 1995; 37:47–52. [PubMed: 7541700]

Salter MG, Fern R. NMDA receptors are expressed in developing oligodendrocyte processes and mediate injury. Nature. 2005; 438:1167–1171. [PubMed: 16372012]

Seeburg PH. The TINS/TiPS Lecture. The molecular biology of mammalian glutamate receptor channels. Trends Neurosci. 1993; 16:359–365. [PubMed: 7694406]

Stout JC, Ellis RJ, Jernigan TL, Archibald SL, Abramson I, Wolfson T, McCutchan JA, Wallace MR, Atkinson JH, Grant I. HIV Neurobehavioral Research Center Group. Progressive cerebral volume loss in human immunodeficiency virus infection: a longitudinal volumetric magnetic resonance imaging study. Arch Neurol. 1998; 55:161–168. [PubMed: 9482357]

Stys PK. White matter injury mechanisms. Curr Mol Med. 2004; 4:113–130. [PubMed: 15032708]

Tang YZ, Carr CE. Development of N-methyl-D-aspartate receptor subunits in avian auditory brainstem. J Comp Neurol. 2007; 502:400–413. [PubMed: 17366608]

Tartaglia MC, Laluz V, Rowe A, Findlater K, Lee DH, Kennedy K, Kramer JH, Strong MJ. Brain atrophy in primary lateral sclerosis. Neurology. 2009; 72:1236–1241. [PubMed: 19349603]

Tekkok SB, Goldberg MP. Ampa/kainate receptor activation mediates hypoxic oligodendrocyte death and axonal injury in cerebral white matter. J Neurosci. 2001; 21:4237–4248. [PubMed: 11404409]

Tomaiuolo F, Di Paola M, Caravale B, Vicari S, Petrides M, Caltagirone C. Morphology and morphometry of the corpus callosum in Williams syndrome: a T1-weighted MRI study. Neuroreport. 2002; 13:2281–2284. [PubMed: 12488811]

Wiltshire K, Foster S, Kaye JA, Small BJ, Camicioli R. Corpus callosum in neurodegenerative diseases: findings in Parkinson's disease. Dement Geriatr Cogn Disord. 2005; 20:345–351. [PubMed: 16192724]

Wohlschlaeger J, Wenger E, Mehraein P, Weis S. White matter changes in HIV-1 infected brains: a combined gross anatomical and ultrastructural morphometric investigation of the corpus callosum. Clin Neurol Neurosurg. 2009; 111:422–429. [PubMed: 19185416]

Wolf HK, Buslei R, Schmidt-Kastner R, Schmidt-Kastner PK, Pietsch T, Wiestler OD, Blumcke I. NeuN: a useful neuronal marker for diagnostic histopathology. J Histochem Cytochem. 1996; 44:1167–1171. [PubMed: 8813082]

Xia Y, Ragan RE, Seah EE, Michaelis ML, Michaelis EK. Developmental expression of N-methyl-D-aspartate (NMDA)-induced neurotoxicity, NMDA receptor function, and the NMDAR1 and glutamate-binding protein subunits in cerebellar granule cells in primary cultures. Neurochem Res. 1995; 20:617–629. [PubMed: 7643968]

Yaldizli O, Glassl S, Sturm D, Papadopoulou A, Gass A, Tettenborn B, Putzki N. Fatigue and progression of corpus callosum atrophy in multiple sclerosis. J Neurol. 2011; 258:2199–2205. [PubMed: 21594686]

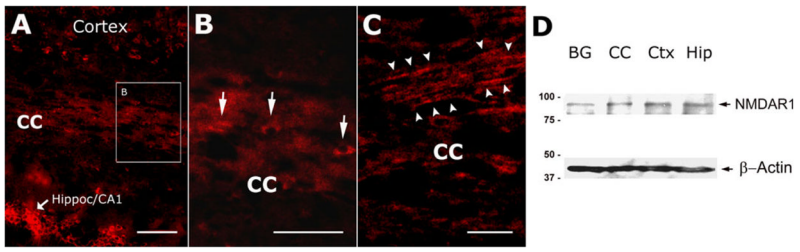

Fig. 1.

A: Location of NMDAR1-like labeling in the CC and remarkable NMDAR1-positive neurons in the hippocampal CA1 region. **B:** High magnification of the boxed area in A. NMDAR1-like immunoreactivities were observed on soma-like structures in the CC (arrows). **C:** Fiber-like structures of the NMDAR1-like immunoreactivities (arrowheads) in the CC adjacent to horizontal corona radiata. **D:** NMDAR1 proteins were detected by Western blot in the CC, BG, Ctx, and Hip. When normalized with β-actin, the NMDAR1 density in the CC was lower than that in Ctx and Hip (data not shown). BG, basal ganglion; Ctx, cerebral cortex; Hip, hippocampus. Scale bars = 50 μm in A, B, 20 μm in C.

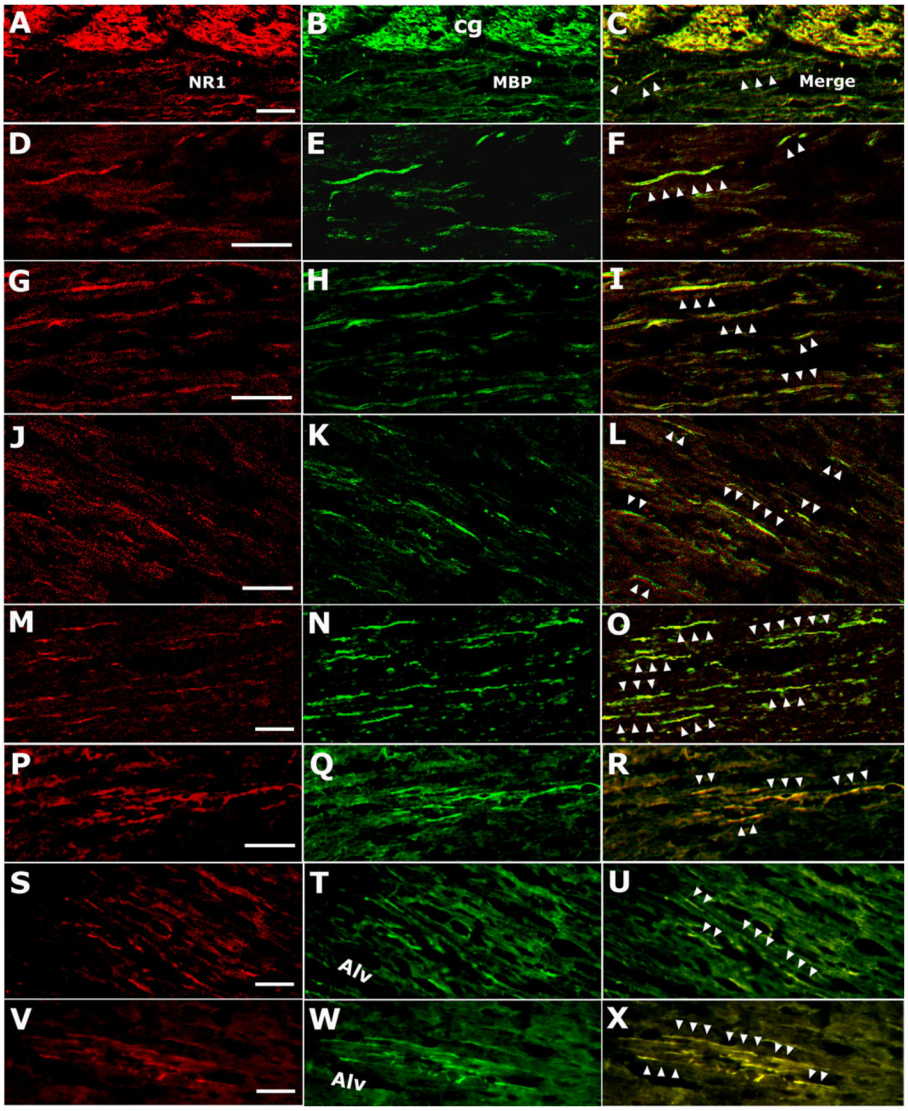

Fig. 2.

Anti-NMDAR1 (NR1; A, D, G, J, M, P, S, V) and anti-MBP (MBP; B, E, H, K, N, Q, T, W) double-labeled (merged; C, F, I, L, O, R, U, X) fiber-like structures observed via confocal microscopy (A–O) and conventional microscopy (P–X). Colocalization of NMDAR1 and MBP is indicated by arrowheads in merged microimages (C, F, I, L, O, R, U, X). In A–F, NMDAR1-positive fibers appear to be from cingulum (cg) regions traveling into the lateral CC. In S–X, NMDAR1-labeled fibers seem to stem from areas of alveolar hippocampus (alv) or from regions around alv, traveling into the lateral CC. All of these microimages are from either lateral CC abutting corona radiata (A–F, J–L, S–U) or corona radiata adjacent to the lateral CC (G–I, M–R, V–X). Scale bars = 20 μm and apply to the rows in which they occur.

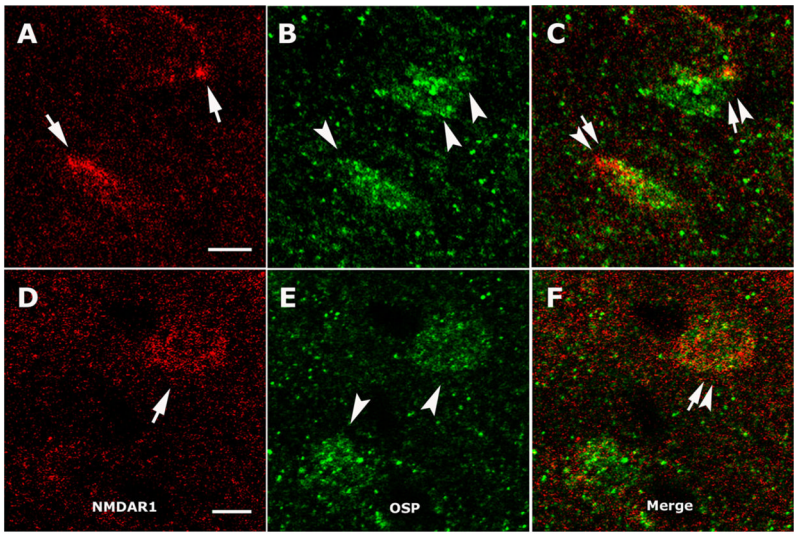

Fig. 3.

Anti-NMDAR1 and anti-OSP double-labeled cells in the CC. **A, D:** NMDAR1-like immunostain (arrows). **B, E:** OSP-positive somata (arrowheads). **C, F:** Double-labeled oligodendrocytes (arrows and arrowheads) after merging. All microimages are from confocal laser scanning microscopic observations. Scale bars = 5 μm and apply to the rows in which they occur.

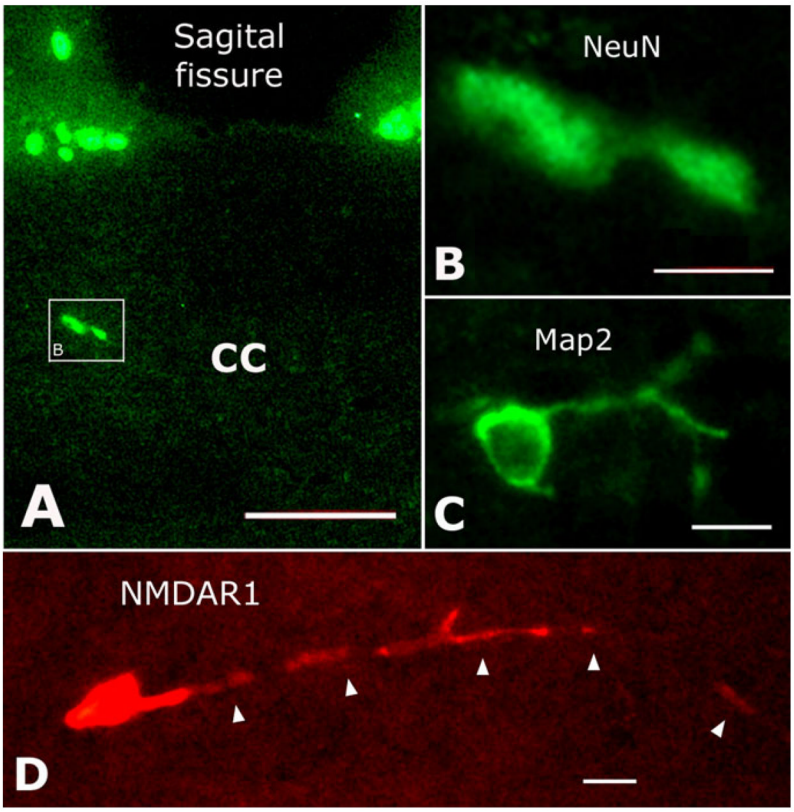

Fig. 4.

Double immunostaining with anti-NMDAR1 and anti-NeuN or anti-MAP2, but no double-labeled structures were observed at all. **A:** NeuN-positive neurons located in the CC. **B:** High magnification of the boxed area in A. **C:** MAP2-labeled neuron in the CC. **D:** NMDAR1-immunostained cell with a long process (arrowheads). Scale bars = 50 μm in A; 15 μm in B–D.

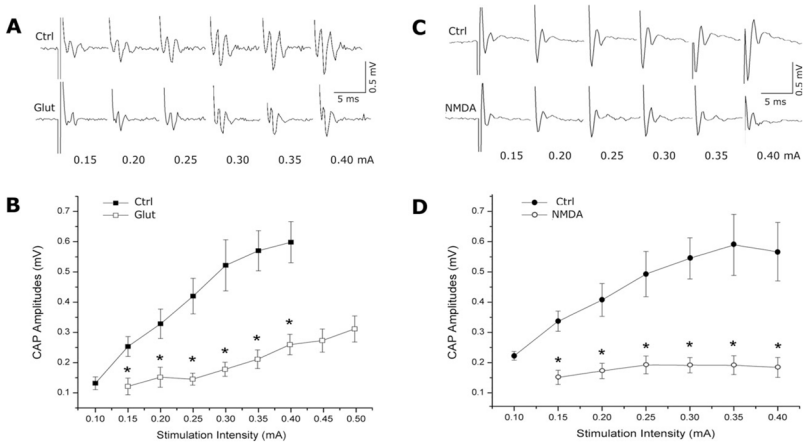

Fig. 5.

Glut- and NMDA-mediated reduction of input–output responses in the CC slices. The CC fiber compound action potentials (CAPs) were evoked by current pulses from 0.1 to 0.5 mA in increments of 0.05 mA. Representative individual CC fiber CAPs recorded from Ctrl and Glut (100 μM)-treated CC slices or from Ctrl and NMDA (100 μM)-treated ones are shown in **A** and **C**, respectively. The average CAP amplitudes recorded from Ctrl CC slices (solid squares) and Glut (open squares) or Ctrl (solid circles) and NMDA-treated (open circles) CC slices were plotted against stimulation intensities (**B, D**). Note that Glut and NMDA significantly reduced the output responses, ★$P < 0.05$ vs. Ctrl; n = 6 in B; n = 5 in D.

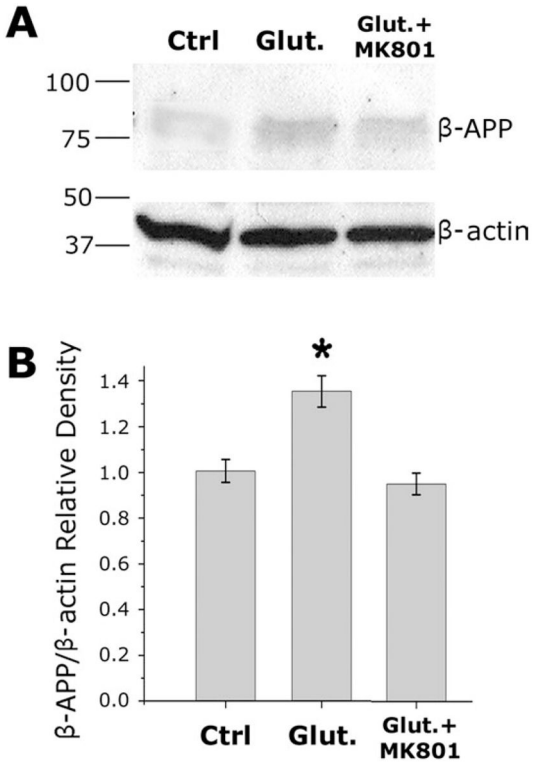

Fig. 6.

MK801 attenuates glutamate (Glut)-induced β-APP accumulation in the CC slices. **A:** Representative Western blot of control (Ctrl; slices incubated in ACSF alone), Glut-treated (50 μM Glut in ACSF), and Glut- + MK801-treated (50 μM Glut and 20 μM MK801) CC slice protein extracts. **B:** Graph displaying β-APP expression comparison of Ctrl, Glut-, and Glut- + MK801-treated groups normalized to β-actin loading control (n = 6, one-way ANOVA; Ctrl vs. Glut: $^{\star}P < 0.05$; Glut vs. Glut + MK801: $^{\star}P < 0.05$; Ctrl vs. Glut + MK801: $P = 0.680$, no difference).